19th Australasian Fluid Mechanics Conference
Melbourne, Australia
8-11 December 2014

Characterisation of interfacial aeration in high-velocity free-surface air-water flows: what does 50% void fraction mean?

S. Felder[1] and H. Chanson[2]

[1]Water Research Laboratory, School of Civil and Environmental Engineering,
UNSW Australia, Manly Vale, NSW 2093, Australia

[2]School of Civil Engineering
The University of Queensland, Brisbane, QLD 4072, Australia

Abstract

High-velocity free-surface flows are complex two-phase flows and limited information is available about the interactions between air and water for void fractions of 50%. Herein a detailed experimental study was conducted in the intermediate flow region on a stepped spillway and the microscopic air-water flow characteristics were investigated. The results showed differences in water and droplet chord times with comparatively larger number of air chord times (0-2 ms), and larger number of water chord times (2-6 ms). A monotonic decrease of chord modes with increasing bubble count rates was observed. Several characteristic time scales were identified based upon inter-particle arrival time analyses of characteristic chord time classes as well as spectral analyses of the instantaneous void fraction signal. Chord times of 3-5 ms appeared to be characteristic time scales of the intermediate flow region having similar time scales compared to turbulent time scales within this region of the flow. A further characteristic time scale of 100 ms was identified in a frequency analysis of the instantaneous void fraction. This time scale was of the same order of magnitude as free-surface auto-correlation time scales suggesting that the air-water flow structure was affected by free-surface instabilities.

Introduction

Air-water flows are commonly observed in hydraulic structures and open channel flows such as spillways, hydraulic jumps and drop structures. In high-velocity free-surface flows, the interfacial aeration occurs naturally from the inception point of free-surface aeration when the outer edge of turbulent boundary layer reaches the free-surface, leading to a complex air-water flow mixture downstream (Figure 1) [2], [11], [14]. Figure 1 illustrates a typical pattern of air-water stepped spillway flows used for the present investigation.

Figure 1. Air-water flows downstream of the inception point of free-surface aeration on a stepped spillway (θ = 26.6°); skimming flow regime; d_c/h = 1.25, q_w = 0.137 m^2/s, Re = 5.5×10^5

In addition, key physical processes include the intense mixing between air and water phases and the interactions with the turbulent flow processes in the various regions of the air-water flow column (Figure 2). On a stepped chute, a significant amount of turbulent energy is dissipated in the lower water column (void fraction < 30%) where interactions with solid boundaries may take place including recirculation movements in the step cavities and unsteady cavity ejection processes, while the upper flow region is characterised by substantial ejections of water droplets in the spray region (void fraction > 70%). In the intermediate flow region (void fraction between 30 and 70%), energetic interactions between air-water and water-air interfaces are observed. This intermediate flow region is characterised by an air-water mixture with a balanced ratio between air and water entities, by collisions, deformations, coalescence and reformations of 'bubbles' and 'droplets'. High bubble count rates, large turbulence levels and large integral turbulent scales were observed in this flow region indicating strong turbulent and energy dissipation.

Despite the important role of this intermediate flow region, detailed information about the air-water flow processes within the intermediate flow region is limited. This contribution aims to characterise the air-water structure and air-water-turbulence interactions in the region of 50% void fraction.

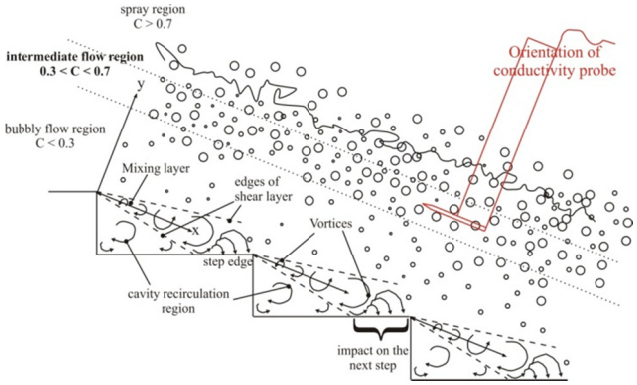

Figure 2. Sketch of stepped spillway skimming flows and positioning of phase-detection probe in the intermediate flow region for 0.49 < C < 0.51

Experimental setup and instrumentation

Air-water flow experiments were conducted on two large size stepped spillway model configurations with channel slope θ = 26.6°, channel width W = 1 m and step heights h = 0.05 and 0.1 m respectively (Figure 1). The air-water flow measurements were conducted for a range of dimensionless discharges 0.69 < d_c/h < 2.22 where d_c is the critical flow depth. The corresponding Reynolds numbers were 8.1×10^4 < Re < 5.7 ×10^5 and the

experimental flow conditions corresponded to the transition and skimming flow regimes [2],[5]. A dual-tip phase detection probe (Ø = 0.25 mm) was positioned at a fixed point while the streamwise air-water interfaces were recorded at 20 kHz for 45 s at least three step edges downstream of the inception point of free-surface aeration (Figure 2).

A typical raw signal output is illustrated in Figure 3 within the intermediate flow region for C ≈ 0.5, where C is the time-averaged void fraction. The raw signal was analysed with a single threshold technique using the distinctive peaks of the bimodal distribution of the raw voltage signals [1]. The threshold was set at 50% of the difference in the two voltage peaks at every location allowing the identification of the time that the probe tip spent in air and in water. The resulting instantaneous void fraction time series were used to calculate the time-averaged void fraction C, the bubble count rate F, the air bubble and water droplet chord times, and the streamwise inter-particle arrival time. The bubble frequency F was defined as the number of water-to-air interfaces per unit time. The air bubble and water droplet chord times characterised the time between the changes of instantaneous void fractions representing characteristic streamwise air/water sizes [5]. The inter-particle arrival time provided information about the randomness of the travelling particles with chord sizes for which a similar behaviour may be expected [3],[6]. Further investigations were based upon the spectral analyses of the instantaneous void fraction signals.

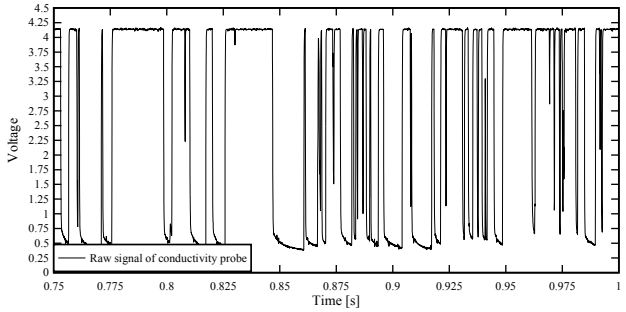

Figure 3. Raw Voltage signal of a phase detection conductivity probe (Ø = 0.25 mm): $d_c/h = 1.28$; $q_w = 0.143$ m^2/s; Re = 5.7×10^5

Characterisation of air-water flows with C = 50%

Air bubble and water droplet chord times

The probability distribution functions of air and water chord times are illustrated in Figure 4 for measurement locations with C = 0.50 (+/- 0.01). Significant differences were observed depending upon the step heights, while the characteristic bubble count rate F_{50} for C ≈ 0.50 presented several trends. Herein the chord time distributions were grouped into characteristic groups summarising the chord times for the stepped spillway with h = 0.05 m in Figures 4A as function of the characteristic bubble count rate F_{50}, and for steps with h = 0.10 m (Figure 4B).

For all data, differences between air and water chord time distributions were observed with a larger amount of smaller air chord times of about 0-1 ms. The numbers of water chords were proportionally slightly larger for chord times between 2 to 6 ms (Figure 4). The differences between PDF distributions of air bubble and water droplet chord times indicated differences in chord times for positions with identical number of detected particles. Toombes and Chanson [12] used surface wave modelling to show the effects of surface waves upon the air bubble chord sizes. The present differences between air and water chord times might partly be linked to some periodic variation of the pseudo-free-surface, affecting the distribution of air-water interfaces in the intermediate flow region.

The present findings suggested some relationship between the characteristic bubble count rate F_{50} and the mode tch_{mode} of chord time PDF distributions. For all data, the relationship between F_{50} and tch_{mode} is illustrated in Figure 5. The observations indicated a monotonic decrease in chord time mode with increasing bubble count rate (Figure 5). A rough estimate of the relationship was given by a power law:

$$tch_{mod\,e} = 30.8 \times F_{50}^{-0.916} \quad (1)$$

Note that the number of data was limited and the inclusion of further data sets with 50% void fraction might provide more details about the relationship.

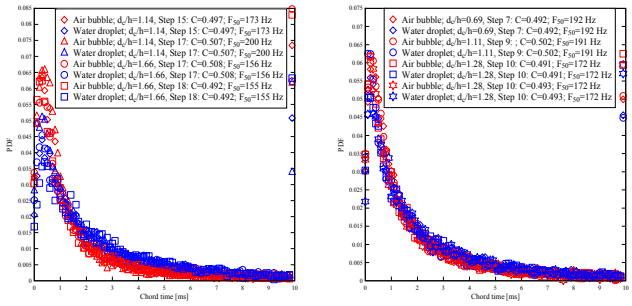

(A) Chord times for 150 Hz < F_{50} < 200 Hz; h = 0.05 .cm

(B) Chord times for 170 Hz < F_{50} < 200 Hz; h = 0.10 m

Figure 4. Probability distribution functions of air and water chord times for void fractions of C = 50% (+/- 0.01)

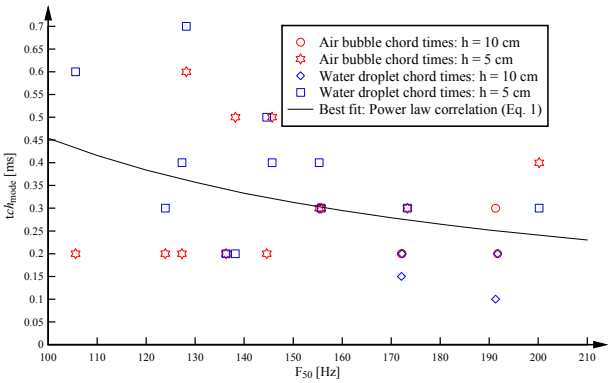

Figure 5. Dimensionless relationship between mode of the chord time PDF and bubble count rate F_{50} with C = 0.50 (+/- 0.01); Comparison with equation (1)

Inter-particle arrival times

The inter-particle arrival time is defined as the time between the arrival of two consecutive 'bubbles' or 'droplets' recorded by a probe sensor fixed in space. The distribution of inter-particle arrival times provides some information on the randomness of the two-phase structure. Ideally, random dispersed flows are driven by a superposition of Poisson processes of particle sizes [6], and any deviation from a Poisson process indicates some unsteadiness and particle clustering [4]. The inter-particle arrival times were herein analysed for five different chord time classes. Typical results are shown in Figure 6 for two different chord time classes and for air and water entities. Little differences in inter-particle arrival time PDFs were observed between air and water chord time distributions for most chord time classes. Differences were however observed for the chord time classes 3-5 ms (Figure

6B), showing a larger number of smaller inter-particle arrival times for the water droplet chord times. These differences were associated with different numbers of 'bubbles' and 'droplets' within this chord time class and the number of air chords was about 40-60% of the number of water chords. No such difference was observed for all other chord time classes. The finding was observed for all data in transition and skimming flows independently of step heights. The shapes of the inter-particle arrival time distributions were affected by the number of particles in a chord time class. A larger number of particles resulted in a proportionally larger number of smaller inter-particle arrival times.

The reason for the differences for the chord time class 3-5 ms remains not known, although it is in agreement with the observations of a comparatively larger number of droplets with chord times of 2-6 ms (Figure 4). The observations of the inter-particle arrival time distributions for similar chord times were consistent with these findings.

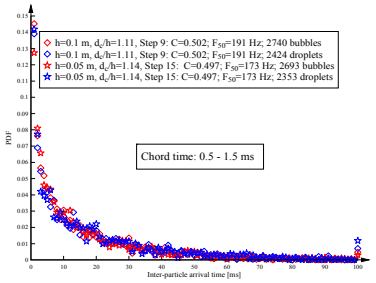

(A) Chord time class 0.5-1.5 ms

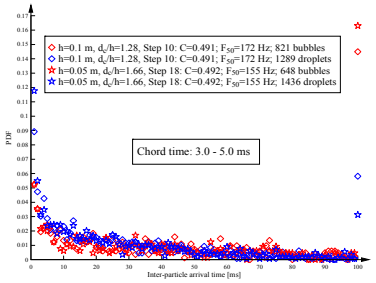

(B) Chord time class 3.0-5.0 ms

Figure 6. Inter-particle arrival times for characteristic air bubble and water droplet chord time classes. Data for C = 0.50 (+/- 0.01)

Spectral analyses of instantaneous void fractions

Spectral analyses were conducted on the instantaneous void fraction signals to identify characteristic frequencies associated with the air-water flows for C = 0.50 +/- 0.01. For each data set, the FFT analysis was conducted for 13 non-overlapping intervals of 65,536 (= 2^{16}) points and the curves were averaged (Figure 7). Further sensitivity analyses were conducted using a number of filters and smoothing techniques. Little effects on the characteristic frequencies were observed and the ensemble averaging was suitable (Figure 7).

Figure 7 illustrates a typical power spectrum density function of the instantaneous void fractions for a data set with C = 0.50 +/- 0.01. In Figure 7, the black curve is the ensemble averaged data. All curves showed a range of characteristic frequencies between 0.9 and 100 Hz with various peak levels within this frequency range (Figure 7). The results differed substantially to observations in the bubbly flow region [9]. For all data, the dominant characteristic frequencies and the corresponding PSD were recorded. The characteristic frequencies are summarised in Figure 8 as functions of the corresponding power spectrum density (PSD) maxima. The results showed a consistent trend for all data sets, illustrated by the median curve (Figure 8). A distinctive frequency of about 9-10 Hz was found in the intermediate region with C = 0.50 (+/- 0.01). Similar specific frequencies were observed in probability distribution functions of the PSD values with bin sizes of 1 Hz and 3 Hz respectively (not illustrated herein).

The present observation was significant since the characteristic frequencies observed in the PSDs identified a range of dominant time scales of the interactions within the intermediate flow region for C = 0.50 (+/- 0.01). The present findings showed a wide range of characteristic frequencies within a range of 2 to 100 Hz, with a distinctive frequency for about 9-10 Hz. That is, the interactions between the air-water interfaces were most energetic with relatively slow fluctuating processes of about 0.1 s time scale. With increasing frequency, and decreasing time scale, the PSD function maxima decreased monotonically (Figure 8) indicating a smaller contribution of the fast fluctuating interactions on the air-water interfaces. The PSD density function for frequencies smaller about 10 Hz showed a decrease in PSD maxima with decreasing frequency.

Overall, the air-water interactions in the intermediate flow region were mostly characterised by relatively slow fluctuating processes, rather than very fast, rapid interactions between air bubbles and water droplets. The present findings showed a first insight into the complex air-water interactions in the intermediate flow region, especially for 50% void fraction. The most energetic time scales were comparatively slow.

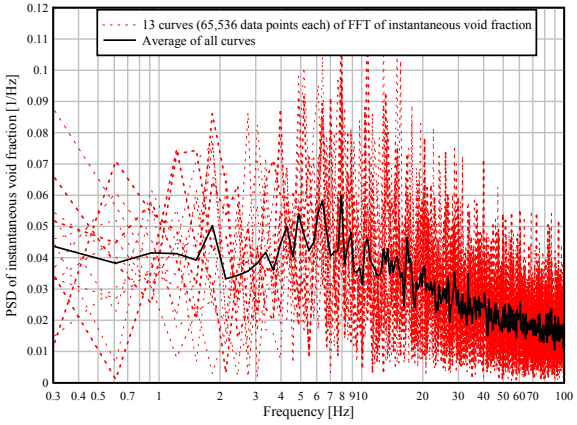

Figure 7. Spectral analysis of the instantaneous void fraction signal for void fractions of C = 0.50 (+/- 0.01)

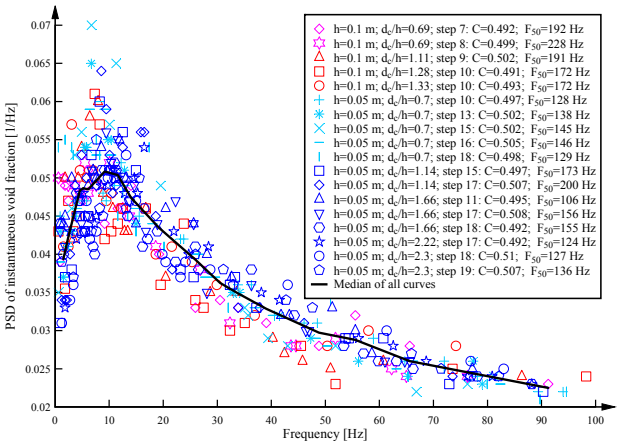

Figure 8. Summary of characteristic frequencies and corresponding power spectrum densities (PSDs) of the instantaneous void fraction signals for void fractions of C = 0.050 (+/- 0.01)

Discussion

The analysis of instantaneous void fraction data with C = 0.50 (+/- 0.01) provided a number of characteristic air-water time scales which might be relevant for the interactions between air-water interfaces. Table 1 summarises these characteristic time scales (upper half), while further time scales observed on the same stepped spillway models are listed. The chord times of 3-5 ms might represent a characteristic time scale associated with the interaction of air and water entities in the intermediate flow region. Such chord time scales were of similar magnitude as the auto- and cross-correlation time scales and integral turbulent time scales observed in the intermediate flow region [7].

The spectral analyses of instantaneous void fractions identified a range of characteristic frequencies between 2 and 100 Hz, independently of the flow regime and of the step heights, for C = 0.50 (+/- 0.01). Frequencies of 10 Hz were the most energetic frequencies, corresponding to a time scale of 0.1 s. This time scale was two orders of magnitude larger than the characteristic integral turbulent time scales within the intermediate flow region. In other words, the characteristic time scale of instantaneous void fraction signal was possibly linked to large scale free-surface fluctuations rather than to the air-water interactions on a sub-millimetric level. Free-surface measurements with acoustic displacement meters in the aerated flow region identified free-surface auto-correlation time scales of a similar order of magnitude [8]. It is believed that this agreement confirmed the effect of free-surface movements upon the air-water flow properties as reported previously [12], [13].

In contrast, cavity ejection frequencies of about 0.2-1 Hz were found on a stepped spillway with $\theta = 26.6°$ [10]. They differed from the characteristic frequencies in the intermediate flow region which indicated that the cavity ejection processes did not impact upon the air-water flow structure in the intermediate flow region.

Time scale [ms]	Comment
3–5	Differences in inter-particle arrival times for air bubble and water droplets ($C \approx 0.50$)
100	Time scale based upon FFT analysis of instantaneous void fraction ($C \approx 0.50$)
3–4	Maximum integral turbulent time scale in a cross-section for $0.3 < C < 0.7$ [7]
4–5	Maximum auto- and cross-correlation time scales in a cross-section for $0.3 < C < 0.7$ [7]
50–200	Free-surface auto-correlation time scales in air-water flows ($C > 0.7$) [8]
1000–5000	Time scales of characteristic cavity ejection frequencies ($C < 0.3$) [10]

Table 1. Summary of characteristic time scales in the intermediate flow region (C = 0.50 (+/- 0.01)). Air-water flow measurements on flat stepped spillways with $\theta = 26.6°$

Conclusion

Air-water flow experiments were conducted in high-velocity free-surface flows on a stepped spillway, with a focus on the detailed air-water interactions in the flow region with same amount of air and water phases: i.e., C = 0.50 (+/- 0.01). Several processing techniques of the instantaneous void fraction signal provided estimates of characteristic time scales. Particle chord times of 3-5 ms might represent a characteristic time scale associated with the interaction between air-water and water-air interfaces in the intermediate flow region, and such time scales were of similar magnitude to the integral turbulent time scales. A distinctive frequency of about 10 Hz was identified using spectral analyses of the instantaneous void fraction signals. The corresponding time scale of 0.1 s appeared to be linked with large scale free-surface fluctuations. Such a magnitude was similar to free-surface auto-correlation time scales indicating that the air-water flow structure might be affected by free-surface waves. Altogether, the air-water flow processes within the intermediate flow region remain poorly understood and further research is needed.

References

[1] Cartellier, A. and Achard, J.L. Local phase detection probes in fluid/fluid two-phase flows. *Rev. Sci. Instrum.*, **62**, 1991, 279-303.

[2] Chanson, H., *The Hydraulics of Stepped Chutes and Spillways*, Balkema, Lisse, 2001.

[3] Chanson, H., Bubbly flow structure in hydraulic jump, *Europ J of Mechanics B/Fluids*, **26**, 2007, 367-384.

[4] Chanson, H., and Carosi, G., Advanced Post-Processing and Correlation Analyses in High-Velocity Air-Water Flows, Environmental Fluid Mechanics, **5**, 2007, 495-508 (DOI 10.1007/s10652-007-9038-3)

[5] Chanson, H. and Toombes, L., Air-Water Flows down Stepped chutes: Turbulence and Flow Structure Observations., *Intl J Multiphase flow*, **28**, 2002, 1737-1761.

[6] Edward, C.F. and Marx, K.D. Multipoint Statistical Structure of the Ideal Spray, Part II: Evaluating Steadiness using the Interparticle Time Distribution, *Atomic Sprays Mech*, **5**, 1995, 435-455.

[7] Felder S., Air-Water Flow Properties on Stepped Spillways for Embankment Dams: Aeration, Energy Dissipation and Turbulence on Uniform, Non-Uniform and Pooled Stepped Chutes., *PhD thesis*., University of Queensland, Australia 2013.

[8] Felder, S. and Chanson, H., Air–water Flows and Free-surface Profiles on a Non-uniform Stepped Chute. *J Hydraul Res*, **52**, 2014, 253-263.

[9] Gonzalez, C.A., An Experimental Study of Free-Surface Aeration on Embankment Stepped Chutes, *Ph.D. thesis*, University of Queensland, Australia, 2005.

[10] Guenther, P., Felder, S. and Chanson, H., Flow Aeration, Cavity Processes and Energy Dissipation on Flat and Pooled Stepped Spillways for Embankments, *Environ Fluid Mech*, **13**, 2013, 503-525.

[11] Rao, N.S.L. and Kobus, H.E., *Characteristics of Self-Aerated Free-Surface Flows, Water and Waste Water/Current Research and Practice*. Vol.10, Eric Schmidt Verlag, Berlin, 1971.

[12] Toombes, L. and Chanson, H., Surface waves and roughness in self-aerated supercritical flow, *Environ Fluid Mech*, **7**, 2007, 259-270.

[13] Wilhelms, S.C. and Gulliver, J.S., Bubbles and waves description of self-aerated spillway flow, *J Hydraul Res*, **43**, 2005, 522-531.

[14] Wood, I.R. *Air Entrainment in Free-Surface Flows.* IAHR Hydraulic Structures Design Manual No. 4, Balkema Publ., Rotterdam, 1991.